Article

Trade Networks in the Neighbouring Roman Provinces of Aquitania-Tarraconensis on the Bay of Biscay: Evidence from Petrographic and Chemical Analyses of Common Coarse Ware Pottery

Ainhoa Alonso-Olazabal [1,*], Maria Cruz Zuluaga [1], Ana Martínez-Salcedo [2], Milagros Esteban-Delgado [3], Maria Teresa Izquierdo-Marculeta [4], François Rechin [5] and Luis Ángel Ortega [1,*]

[1] Department of Geology, University of the Basque Country (UPV/EHU), Sarriena s/n, 48940 Leioa, Spain; mcruz.zuluaga@ehu.eus
[2] Sociedad para el Estudio de la Cerámica Antigua en Hispania (SECAH), P.O. Box 33, 28086 Madrid, Spain; arkeon@euskalnet.net
[3] Faculty of Social and Human Sciences, University of Deusto, Mundaiz Kalea 50, 20012 Donostia, Spain; milagros.esteban@deusto.es
[4] Basque Cultural Heritage Centre, Basque Government, Donostia-San Sebastian Kalea 1, 01010 Vitoria-Gasteiz, Spain; maite.izmar@gmail.com
[5] ITEM (UR 3002), Université de Pau et des Pays de l'Adour, Av. du Doyen Poplawski, 64000 Pau, France; francois.rechin@univ-pau.fr
[*] Correspondence: ainhoa.alonso@ehu.eus (A.A.-O.); luis.ortega@ehu.eus (L.Á.O.)

Abstract: Common non-wheel-thrown Roman pottery from the southern Aquitania and north-eastern of Tarraconensis provinces (CNT-AQTA) of the Early and Later Roman Empire (1st to 5th centuries AD) has been studied. Petrological, mineralogical, and chemical analyses were conducted to contrast with the archaeological study of the pottery. The chemical composition of many pottery samples displays different patterns of burial chemical modification, limiting their use for provenance and diffusion studies. Particular emphasis has been paid to the petrographic features of the fabrics, as they do not change during burial, reflecting the nature of the raw material and making it possible to identify the provenance areas of the raw materials. Around the Bay of Biscay, the same pottery tradition continued in the neighbouring provinces during Roman times. Petrographic studies make it possible to determine the distribution of pottery and the changes in trade networks during the Roman period across the area of the Bay of Biscay being studied.

Keywords: coarse pottery; burial chemical modifications; provenance areas; trade networks; Bay of Biscay; Roman Empire

1. Introduction

Pottery is an important source for the reconstruction of the socio-economic framework of different periods and cultures since it provides clues not only about technological skills, but also about cultural and trade networks [1–3]. The Roman period is a particularly good example of how the analysis of pottery distribution reveals patterns of exchange and interaction between different areas or societies. At Roman sites in the Mediterranean and Atlantic regions, both fine and coarse wares are profuse, revealing trade between the Mediterranean Sea and Atlantic Ocean and evidencing not only long-distance movements but also cross-border trade relations.

The Roman occupation of the neighbouring areas of the northern Iberian Peninsula and southern France is well documented by numerous archaeological excavations carried out in this geographic area [4–12]. The communication network, by both terrestrial and maritime routes, linking the Cantabrian coast to the rest of the Roman world, is well

known [13–19]. The connection between the Cantabrian coast and the coasts of Aquitaine and Brittany was mentioned by Caesar (CAES. Gal.3.26.6), Strabo (STR. 3.4.18) and Orosius (OROS. Hist.6.21.4) in de Soto [20]. Important harbours such as *Oiasso* (Irun), *Lapurdum* (Bayonne) and *Burdigala* (Bordeaux) as well as secondary harbours in rivers and estuaries (e.g., *Portus Amanum-Flaviobriga* in Castro Urdiales, Forua in Gernika, Zarautz, Donostia and Hondarribia) have been identified for the trade of goods (e.g., wine, fish products, lard, broad beans and mineral resources). All of them articulated a network of ports that guaranteed maritime communications around the Bay of Biscay [21–26]. The maritime route was active together with the main continental roads of *Ab Asturica-Burdigalam* and secondary routes crossing the Pyrenees, *Tarraco-Oiasso* and *Pisoraca VI-Portu Amamus*. Maritime, waterway, and continental routes constitute the main trading communication network operating in the eastern Cantabrian region, linking the Roman provinces of Aquitania and Tarraconensis. In this way, the northeast of Hispania was fully integrated into the framework of Roman trade across the Cantabrian Sea.

The most frequent type of pottery found at Roman sites on the Bay of Biscay (*Sinus Aquitanicus*) was the common non-wheel-thrown pottery, known as "cerámica común no torneada Aquitano-Tarraconensis" (CNT-AQTA) [27]. This type of pottery occurs at all sites on the Cantabrian coast, in Aquitaine and in the middle and upper Ebro valleys [4,27,28]. Very few studies about this coarse pottery have been carried out due to its rough appearance and lack of aesthetic appeal. However, in recent decades, interest in this type of pottery has increased due to its multiple uses in everyday activities, allowing coarse pottery to be used as a tool for assessing the way of life in Roman settlements.

The studied pottery was collected from sites in the neighbouring imperial provinces of Tarraconensis and Aquitania, in different administrative districts, but within the organisational framework of the Roman state. Some sites were associated with productive activities (Arbiun) or funerary activities (Santa Elena). Other sites correspond to different settlement models: urban centres (Iruña/Veleia), *civitas Aqvensium* (Dax) or *Lapurdum* (Bayonne), rural settlements or *villae* (Aloria, Lalonquette and Pardies). Small temporary settlements (Moliets) and coastal enclaves with industrial and maritime activities (Forua, Santa María la Real and Zarautz-Jauregia) were also considered. Finally, the Santiagomendi site represents the transition from the pre-Roman way of life to the new Roman socio-economic, political and cultural patterns [29,30].

Mineralogical, petrographic, and chemical analyses were conducted to support the archaeological study based on the examination of ware shape, style, colour, decoration, and the overall fabric of the pottery. Petrographic, mineralogical, and chemical characterisation can provide significant information on raw material provenance and potentially the technology involved in the manufacturing process. The aim of this study is to assess the petro-mineralogical and geochemical composition to determine differences in the composition and provenance of Roman coarse pottery, to define an accurate distribution pattern and to establish connections with different Roman period productions (1st–5th AD centuries) to trace the evolution of trade networks around the Bay of Biscay.

2. Geological Background

The structure and geology of the studied region are highly complex as a result of the convergence of the Iberian and Eurasian plates during the Cretaceous-Miocene. The Bay of Biscay and the western Pyrenean domains represent a strongly structured region as a consequence of consecutive extensive and compressive tectonic cycles that started in the early Palaeozoic. The Palaeozoic basement complex, known in the studied area as the Palaeozoic Basque Massifs: Aldudes, Cinco-Villas and Ursuya massifs, is formed by Ordovician to Carboniferous sedimentary rocks, limestones, sandstones and shales where Permian Aya granite and andesite dykes intruded, and the Ursuya massif consists of high-grade granulites, paragneisses and migmatites. During the Permian-Early Triassic, a red detrital unit was deposited in extensional conditions with abundant volcanic materials. Later Triassic to Jurassic rift events developed the formation of intracontinental

basins filled by thick sequences of siliciclastics, carbonates, and evaporites with associated mantle-derived intrusions, ophites. The latest Triassic and Jurassic marine transgression resulted in marls and limestone deposits. During the early Cretaceous, extension led to the development of several troughs that consist of limestones, sandstones and marls that are surrounded by continental and platform domains covered by thick fluvial to deltaic sandstones and marls, and shallow marine limestones. Extreme crustal thinning in the Bay of Biscay led to the exhumation of the subcontinental mantle and resulted in continental breakup and seafloor spreading initiation. This event was recorded by the deposition of deep marine sediments and was accompanied by alkaline magmatism, both intrusive and volcanic, from the late Aptian to the early Santonian.

The beginning of compressional deformation is marked by a regional unconformity in Santonian sediments. The transition from post-rift to syn-orogenic evolution is recorded by the deposition of siliciclastic turbidites dated from the Cenomanian to the Eocene, topped by Oligocene sandstones, conglomerates and evaporites. The major collision phase was reached during the Eocene and continued until the end of the Oligocene with the generalised uplift of the chain and the formation of foreland basins. Between the late Miocene and the early Pleistocene, in the north Pyrenean foothills, the last main fluvial depositional stage occurred with siliciclastic fan deposits fed by the erosion of the Pyrenees and the Massif Central. During the Pleistocene, foothills underwent strong incisions on stage, developing alluvial sheets, some of them controlled by glacial pulses. The climatic alternations, oscillations in sea level and a succession of episodes of excavation and filling in the hydrographic network promoted the tiering of alluvial terraces along the rivers, and the north-westerly winds developed dune deposits along the Atlantic edge [31–33].
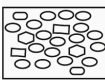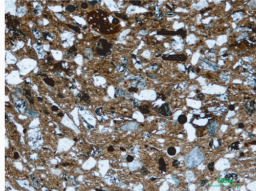
3. Materials and Methods

3.1. Materials

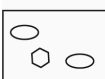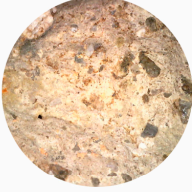The pottery included in the present study corresponds to Roman non-wheel-thrown pottery productions from different archaeological sites in the eastern Cantabrian region (Spain) and southern Aquitaine (south France) on the Bay of Biscay (Figure 1). The pottery analysed corresponds to rough, handmade domestic pottery, mainly used for everyday activities (cooking, table and storage ware). This unsophisticated pottery, coarse and essentially functional, lacks major changes in form and stylistic evolution over the course of the centuries.

The selected samples correspond to the most representative and profusely common non-wheel-thrown pottery productions at the studied sites. The macroscopic analysis based on the abundance and grain-size of 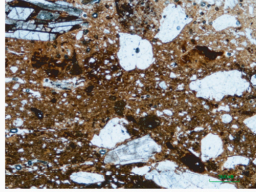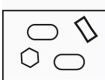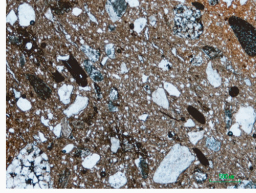inclusions, firing conditions, hardness, fracture, compaction, and finishing allowed us to classify the potteries into three main groups, named G1, G2 and G3 productions [4,28,29,34]. G1 production (86 potsherds) is composed of grey (7.5R 6/0, 7.5R 5/0), with some superficial patches of reddish-yellow (5YR 5/8) and light red (2.5YR 6/8). This production shows medium sand grains with well-sorted white, grey, black, reddish, golden and silver rounded inclusions (0.5–2 mm). The fabric is hard and rough, with a smooth fracture. The G2 production (45 sherds) is composed of various grey (7.5R 4/0; 7.5R 5/0), grey-pink (7.5YR 6/2) and yellow-reddish (5Y 6/6) bodies with scarce voids. This medium-coarse sand-grained (0.5–3 mm) fabric is characterised by poorly sorted white, grey, brownish, blackish, reddish, and silver inclusions. The fabric is hard and rough, with a smooth fracture. The G3 group (55 potsherds) is reddish-orangish (5YR 5/6; 2.5YR 5/8) coloured at the external borders and grey (7.5R 6/0; 7.5R 5/0) coloured in fresh cuts or the internal body. Medium-coarse sand-grained (0.5–3 mm) fabric is characterised by poorly sorted white, grey, silver, and golden inclusions with voids. The inclusions are different in type, abundance, and size. The fabric is hard and rough, with smooth fractures. The studied G1, G2 and G3 groups correspond to the G3, G1 and G2 pottery groups described by Martínez-Salcedo [34]. A total of 186 potsherds were selected for the archaeometric analyses from eight Tarraconensis archaeological sites and eight Aquitania

sites. The main distinguishing features are summarised in Figure 2 and correspond to various types of wares, mainly pots, plates, jars and bowls (Table S1).
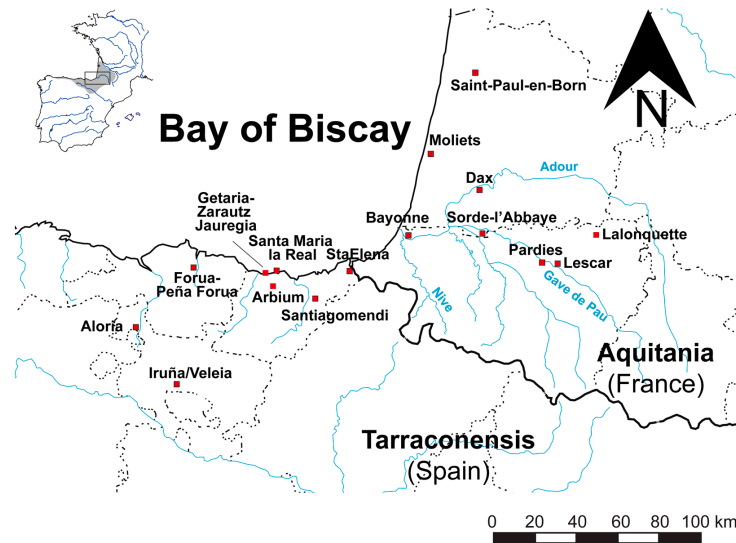
Figure 1. Geographic location of the archaeological sites where samples were analysed around the Bay of Biscay: sites of Aloria (Amurrio, Araba); Iruña-Veleia (Iruña de Oca, Araba); Forua-Peña Forua (Forua, Bizkaia); Getaria-Zarautz Jauregia (Getaria, Gipuzkoa); Santa Maria La Real (Zarautz, Gipuzkoa); Arbium (Zarautz, Gipuzkoa); Santa Elena (Irun, Gipuzkoa); Santiagomendi (Astigarraga, Gipuzkoa) in Tarraconensian province, Spain. Sites of Saint-Paul-en-Born (Landes, Nouvelle-Aquitaine); Moliets-et-Maa (Landes); Bayonne (Nouvelle-Aquitaine); Dax (Landes, Nouvelle-Aquitaine); Lalonquette (Pyrénées-Atlantiques, Nouvelle-Aquitaine); Pardies (Peyrehorade, Landes); Sorde-l'Abbaye (Landes, Nouvelle-Aquitaine); Lescar (Pau, Nouvelle-Aquitaine) in Aquitanian province, France.

Production	Fresh sample photographs	Photomicrographs	Observations
G1			**Macroscopic**: Greyish colour pottery fabric with white, grey, reddish and greyish colour. Inclusions size: 0.5 – 2 mm **Microscopic**: Polygenic fine-grained rock fragments well-ordered distributed
G2			**Macroscopic**: Greyish to yellow-reddish colour pottery fabric with white, black, reddish and greyish colour. Inclusions size: 0.3 – 3 mm **Microscopic**: Igneous felsic rock and high-grade metamorphic fragments
G3			**Macroscopic**: Greyish colour pottery fabric with white, grey, reddish and greyish colour inclusions. Reddish colour outside. Inclusions size: 0.5 – 2 mm **Microscopic**: Polygenic, coarse-grained, randomly distributed rock fragments

Figure 2. Synoptic sketch of macroscopic and microscopic features of the three main pottery productions. Fresh sample photographs: diameter corresponds to 1 cm. Photomicrographs: width of field corresponds to 2.4 mm. Geometric symbols in the synoptic sketch correspond to inclusions of different compositions.

3.2. Methods

The petrographic study was performed on thin sections using a Nikon Eclipse LV100pol polarised light microscope equipped with a DSF-11 digital camera and DSL-2 control unit at the Laboratory of the Department of Geology, University of the Basque Country (UPV/EHU). Each thin section was analysed under plane and cross-polarised transmitted light to evaluate the mineralogy and clay matrix characteristics according to [35,36], with special attention to some aspects described in [37–39].

Chemical composition analysis of mineral inclusions was carried out on polished carbon-coated thin sections using a JEOL JSM-6400 Scanning Electron Microscope (SEM) (JEOL, Tokyo, Japan) equipped with an INCA EDX detector X-sight Series Si (Li) Oxford pentaFET microanalysis system.

Pottery mineralogical composition was analysed by X-ray diffraction (XRD) using a Philips X'Pert diffractometer (Malvern PANalytical, Almelo, The Netherlands) equipped with graphite monochromator adjusted to Cu-k$_{\alpha1}$ X-radiation operating at 40 kV and 20 mA. The data collection was performed in a continuous scan ranging from 5 to 70° 2θ at acquisition rate of 0.02° 2θ per second. The mineral phase identification and semi-quantitative determinations were performed using X'Pert HighScore Plus 3.0 software (Malvern PANalytical, Almelo, The Netherlands). Semiquantitative analyses of the mineral phase were obtained using the experimental reference intensity ratio (RIR) for each mineral in the sample.

The major and trace element analysis for pottery sherds was carried out using a Thermo X-Series 2 quadrupole ICP-MS (Thermo Fisher Scientific, Bremen, Germany), after fusion of 250 mg of finely ground sample with 500 mg high-purity grade LiBO2 (analysis grade pure, Corporation Scientifique Claisse) in Pt-Au crucibles, followed by nitric acid dissolution of the melt. The sample preparation and conditions of measurements were performed following the procedure of García de Madinabeitia et al. [40]. All the analyses were carried out at the Advanced Research Facilities (SGIker) of the University of the Basque Country (UPV/EHU).

4. Results

4.1. Petrographic Analysis

The microstructure characteristics, considering amount, grain-size, sorting, roundness and sharpness, as well as the nature of components, allowed the identification of different petrographic fabrics within the three main pottery productions. The abundance and distribution of the petrographic types at the archaeological sites are shown in Figure 3.
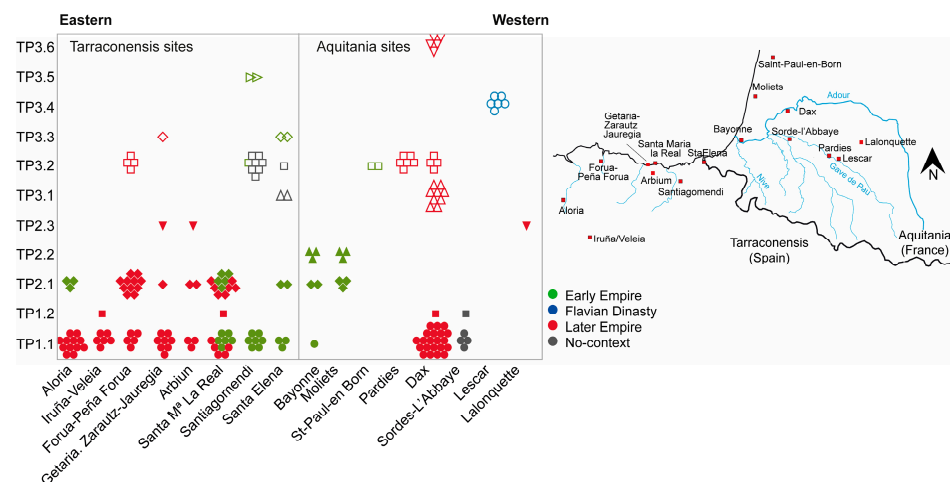
Figure 3. Distribution of petrographic fabrics at the study sites. Each point represents one sample. Right: location of the sites. Each symbol represent a different petrographic fabric.

The G1 fabric group is formed by two petrographic fabrics, TP 1.1 and TP 1.2. The fabric TP 1.1 is highly abundant, comprising 95% of the G1 group of wares (82 samples of $n = 86$ in the G1 assemblage). The fabric shows a very homogeneous matrix/inclusions ratio. The ground is mainly clayey. Pores present a single-spaced related distribution and are oriented parallel to the margins. The nonplastic inclusions (35%–45%) present a closed to single-spaced related distribution and are commonly oriented parallel to the margins. The subangular-subrounded inclusions display typically a unimodal grain size distribution, are well sorted, and have grain sizes ranging between 0.25 and 0.50 mm. The inclusions correspond to a wide variety of rock and mineral fragments. The rock fragments include sedimentary rocks (greywackes, ferruginous sandstones), metamorphic rocks (schists and slates, sometimes with crenulation schistosity, gneisses, high-grade metamorphic rocks with epidote and occasional mylonites), plutonic and volcanic rocks (diorites, basalts and diabases with ophitic/subophitic texture). Within mineral fragments, mono- and poly-crystalline quartz, idiomorphic evaporitic quartz, epidote, plagioclase, perthitic potassium feldspar, amphibole, sparite calcite nodules, micritic nodules, spathic calcite, blackish inclusions and rare biotite laths, pyroxenes, garnets, etc. have been recognised (Figure 4a–c). Some grog fragments are also observed. The fabric TP 1.2 shows similar features to TP 1.1, although it is distinguished by the occurrence of high-sphericity quartz inclusions with a homogeneous grain size (Figure 4d).
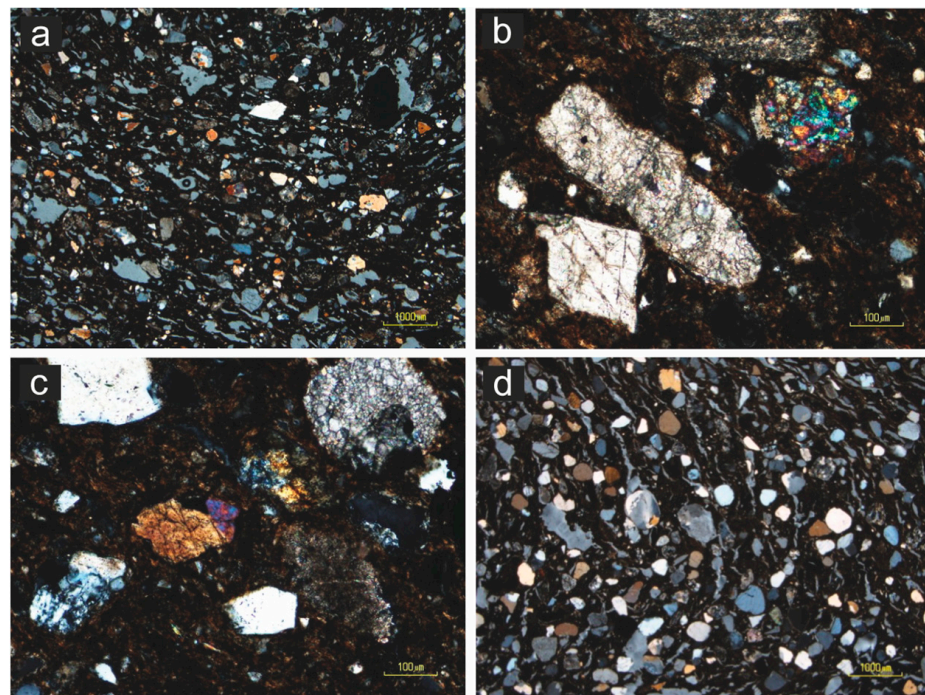

Figure 4. Representative thin section photomicrographs of the G1 fabric ceramic from different sites. (**a**): Fabric TP 1.1 from Arbium site (sample ARBI-10, PPL). (**b**): Inclusions of calcite spar, carbonate fragments and epidote included in TP 1.1 fabric from Bayonne site (sample BAY-36, PPL). (**c**): Calcite, epidote, and pyroxene inclusions of the TP 1.1 fabric from Zarautz site, (SNR-18, PPL). (**d**): Texture of the TP 1.2 petrographic fabric from Dax, (DAX-79-19, XPL), PPL: parallel-polarised light, XPL: cross-polarised light.

The G2 fabric group is composed of three petrographic fabrics. The petrographic fabric TP 2.1 is the most abundant, accounting for 80% (36/45) of the G2 wares. These ceramics are characterised by a fine-grained groundmass varying from clayey to sandy in nature, with angular to subrounded coarse inclusions ranging from 0.5 to 6 mm in size. The pores present a single- to double-spaced related distribution and are oriented parallel to the vessel margin. The number of inclusions ranges between 15% and 25% and their orientation is mainly parallel to the margins, showing poor sorting with a bimodal

grain size distribution. The coarse fraction includes rock fragments mainly of quartz-feldspatic igneous-felsic nature, frequent metamorphic rocks with sillimanite and a few sandstones. In addition, mineral fragments such as mono- and polycrystalline quartz with undulose extinction, potassium feldspar and blackish inclusions are frequent, while muscovite, biotite laths and amphibole are very few. Two end subgroups, or subfabrics, can be distinguished depending on the clayey or sandy nature of the groundmass. The sandy matrix constitutes one of the end subgroups characterised by a bimodal grain size distribution (modes ranging between 0.125–0.25 mm and 0.5–2.0 mm) of mainly subangular quartz-feldspathic inclusions (Figure 5a,b).
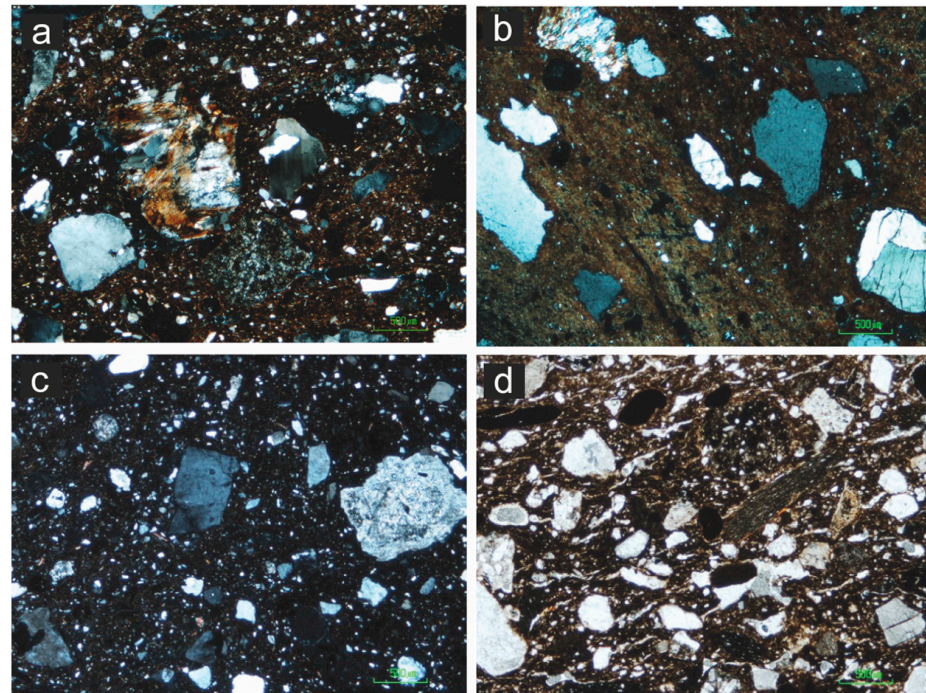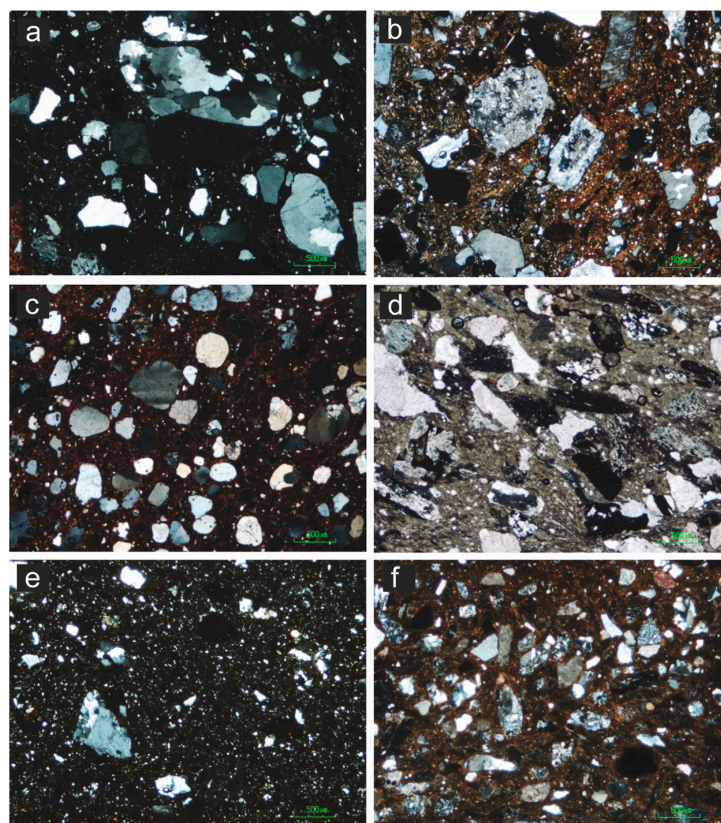

Figure 5. Photomicrographs showing petrographic features of the G2 fabric group. (**a**): Sandy matrix end subgroup showing bimodal distributions of angular inclusions distinctive of TP 2.1 fabric (sample SNR-33, XPL). Note sillimanite-bearing rock fragment at the centre. (**b**): The clayey matrix end subgroup shows coarse angular inclusions of TP 2.1 fabric (sample F-55, XPL). (**c**): Representative TP 2.2 fabric showing sub-rounded to sub-angular quartz with idiomorphic plagioclase inclusions (sample BAY-39, XPL). (**d**): Polygenic character of the TP 2.3 fabric; note the elongated slate fragment (sample GEA-8, PPL); PPL: parallel-polarised light, XPL: cross-polarised light.

The fabric TP 2.2 was only identified at two sites, accounting for 13% (6/45) of the G2 group wares. Depending on the site location of the samples, the groundmass varies between clayey (Moliets site) and sandy (Bayonne site), with pores presenting a single- or double-spaced related distribution and a preferred orientation parallel to the vessel margins. As a rule, the inclusions (15%–20%) show a bimodal grain size distribution with common poorly sorted, subrounded to subangular fine to coarse inclusions of frequent quartz grains and strongly altered feldspars (0.125–0.5 mm), especially idiomorphic plagioclase, the latter being distinctive of this petrographic type. Abundant rounded to angular quartz-feldspar and rare mica inclusions are observed within the fine-grained groundmass. Additionally, rare muscovite-bearing granitic rock fragments, scarce granodioritic as well as sedimentary rock fragments are also observed (Figure 5c).

Only three samples constitute the TP 2.3 petrographic fabric. This fabric is notably polygenic, including a fine-grained (<0.1 mm) quartz-feldspathic and muscovite sandy groundmass, and a medium-coarse fraction (0.25–1.25 mm) including, mainly subangular-subrounded, poorly sorted inclusions of different composition. The coarse inclusions

(30%–40%) display a close-spaced to double-spaced related distribution and a preferred orientation parallel to the vessel margins. The coarse fraction consists of common mono- and polycrystalline quartz, potassium feldspar, altered plagioclase and a few biotite, pyroxene, and calcite aggregates. Additionally, rare rock fragments of different origins are included: slate fragments in the Getaria-Zarautz Jauregia sample, subvolcanic rocks displaying ophitic texture in the Arbiun sample and high-grade metamorphic rocks with sillimanite fragments in the Lalonquete sample (Figure 5d).

The G3 fabric group is the least common at the sites and the most heterogeneous based on petrographic criteria, including six petrographic fabrics. The occurrence of each petrographic fabric is mainly restricted to a single archaeological site. The TP 3.1 fabric includes 11 samples from the Dax and Santa Elena sites. The occurrence of chessboard subgrain patterns in quartz is the distinctive feature of this fabric (Figure 6a). The fabric is characterised by a very fine clayey matrix with a few oriented pores parallel to vessel margins. The moderately sorted coarse fraction (20%–25%) is mainly composed of quartz inclusions of high roundness and sphericity and quartz inclusions of variable grain size (0.25–1.25 mm), in some cases with bimodal distribution. In addition to perthitic potassium feldspar, there is a common occurrence of plagioclase replaced by epidote and brown biotite. More rarely, two-mica granite fragments occur.

Figure 6. Photomicrographs showing petrographic features of the G3 fabric group. (**a**): Petrographic fabric TP 3.1 presenting rounded chessboard pattern quartz (sample DAX-79-3, XPL). (**b**): Idiomorphic plagioclase distinctive of the TP 3.2 fabric (sample F-16, XPL). (**c**): Highly spherical and rounded quartz grains embedded in a very fine clayey matrix distinctive of the TP 3.3 fabric (sample GEA-4, XPL). (**d**): The TP 3.4 fabric includes polygenic inclusions such as slates and schists, biotitic-amphibole granodiorites and sandstones (sample Lescar-10, PPL). (**e**): Clayey matrix with very fine quartz grains with random coarse quartz fragments of TP 3.5 fabric (sample STGR-17, XPL). (**f**): TP 3.6 fabric showing moderately sorted polygenic inclusions (sample DAX-5, XPL). PPL: parallel-polarised light, XPL: cross-polarised light.

Petrographic fabric TP 3.2 is the most numerous and widely distributed fabric in the G3 group and includes 25 samples from Forua-Peña Forua, Santiagomendi, Santa Elena, Saint-Paul-en-Born, Pardies and Dax. The distinctive feature of this fabric is the presence of idiomorphic plagioclase inclusions (Figure 6b) scattered in a clayey-sandy matrix, sometimes rich in micas. The coarse fraction inclusions (15–20%) are subangular to rounded in shape, with variable grain size ranging from very fine to gravel size (0.1–2.5 mm), poorly sorted and arranged in a bimodal grain size distribution. Frequent inclusions were quartz (mono- and polycrystalline), zoned and poorly altered plagioclase, common perthitic potassium feldspar, granite fragments and very few biotite laths and amphibole.

Petrographic fabric TP 3.3 comprises only three samples and occurs at Getaria-Zarautz Jauregia and Santa Elena. The most distinctive feature is the presence of coarse (0.25–0.50 mm) highly spherical and rounded quartz and potassium feldspar inclusions (30–40%), spread in a very fine clayey matrix. They display a moderately sorted, bimodal grain size distribution. Frequent inclusions are mono- and polycrystalline quartz with common altered coarse plagioclase (≤1.3 mm), granitoid fragments or a few slates and ferruginous sandstones (Figure 6c).

Petrographic fabric TP 3.4 includes six samples from the Lescar site. Wares of this fabric show a fine clayey matrix, with few pores parallel to the vessel margin. The polygenic inclusions (25–35%) display a bimodal grain size distribution with a poorly sorted coarse fraction (0.8–2 mm) of angular to subrounded shapes. The nature of the inclusions is diverse, including frequent fragments of metamorphic rocks (frequent slates and schists, some of gravel size > 2 mm), common subrounded igneous rock fragments (amphibole granodiorites, subvolcanic rocks with ophitic textures) and very few sedimentary lithic fragments (sandstones) (Figure 6d).

Only two samples from the Santiagomendi site define the TP 3.5 petrographic fabric. These samples are characterised by a mainly clayey matrix with pores in an open-spaced, related distribution. The nonplastic inclusions (<10%) display an open-spaced related distribution, medium grain size (0.25–0.80 mm) and variable subrounded to subangular shapes, thus defining a poorly sorted fabric with a bimodal grain size distribution. Fragments of granitic rocks and fragments of potassium feldspar, plagioclase and quartz are common (Figure 6e).

Petrographic fabric TP 3.6 includes five samples from the Dax site. This fabric shows petrographic similarities to the TP 1.1 fabric regarding the heterogeneous composition of inclusions. The coarse-grained (0.25–0.5 mm) inclusions (35–45%) reflect a bimodal grain size distribution with poorly to moderately sorted fabric. The angular to subrounded inclusions present a closed- to double-spaced related distribution and correspond to various types of sedimentary, igneous, and metamorphic fragments (Figure 6f).

4.2. X-ray Powder Diffraction

X-ray powder diffraction results agree with the data obtained by mineralogical and petrographic observations. Figure 7 shows a representative diffractogram per pottery fabric group. The samples are composed of quartz, phyllosilicates, feldspars (both plagioclase and potassium feldspar) and minor amounts of calcite and titanium oxides.

Quartz is the most abundant mineral in the three fabric groups, with an average content of 50%. The most homogeneous contents in quartz are found in the G2 group samples, while contents below 30% are observed in some G1 group samples and above 60% in some G3 group samples. Phyllosilicates are the second most abundant minerals, with average values of approximately 40%. Phyllosilicates vary inversely with quartz content, although in some cases variations are related to feldspar and carbonate content. The most significant mineralogical difference between the three fabric groups is related to the minor minerals such as feldspar and calcite. Feldspar content (plagioclase and potassium feldspar) is by far the highest in the G3 fabric samples. The samples from the Moliets, Pardies, Bayonne and Dax sites show above-average feldspar contents. In fact, Moliets samples contain up to 30% plagioclase and up to 10% potassium feldspar. With

respect to calcite, its occurrence is practically limited to samples of the G1 group from Tarraconensis sites, with low contents and rarely exceeding 5%.
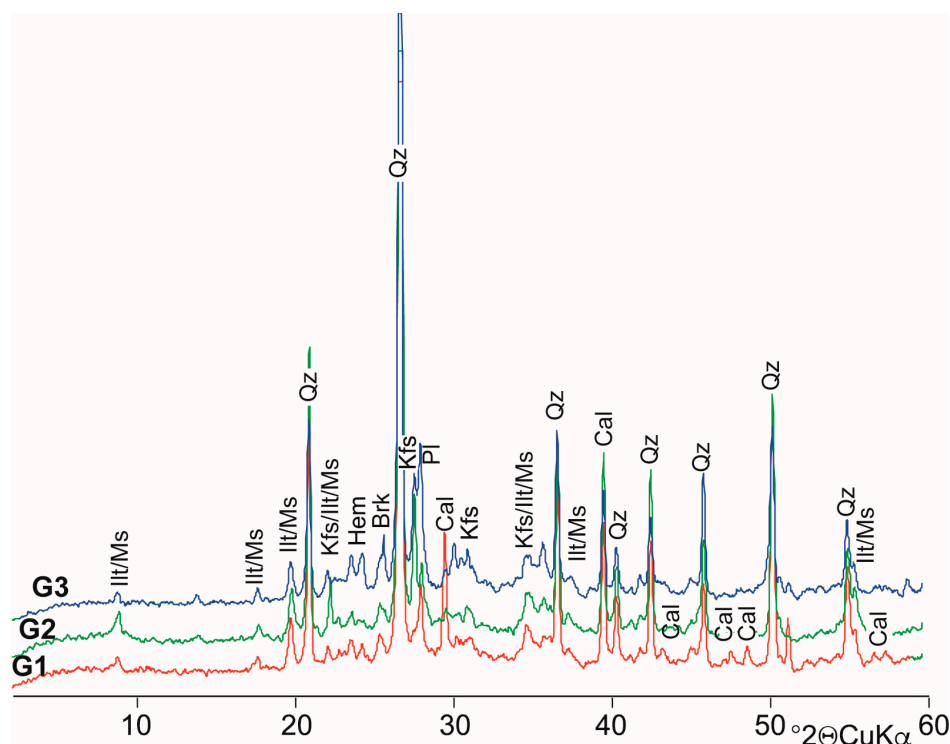
Figure 7. XRD patterns of representative samples for main G1, G2 and G3 pottery fabric groups. Mineral abbreviations after Whitney and Evans [41]: Cal (Calcite), Ilt (Illite), Ms (Muscovite), Kfs (Potasium feldspar), Pl (Plagioclase), Hem (Hematite), Brk (Brookite) and Qz (Quartz).

The XRD mineralogical composition depends on the raw material composition and the firing conditions if secondary phase crystallisation does not occur during burial. The occurrence of calcite in some samples suggests firing temperatures below 800 °C under oxidising conditions [42–44]. Calcite decomposes at temperatures above 700 °C to form gehlenite in clayey materials [43–46]. However, the studied samples show minor contents of secondary calcite filling voids. Therefore, the occurrence of calcite cannot be used to determine firing temperatures. The phyllosilicate breakdown can also be used to estimate firing conditions. Phyllosilicates began to breakdown at 500 °C and completely disappeared upon heating to temperatures > 1000 °C [43,47,48]. Most of the samples are characterised by the existence of (001) phyllosilicate reflexion, indicating that the crystalline structure collapse has not yet started. Samples not showing (001) reflection include all from the Aloria site and some from the Arbiun, Santiagomendi, Santa Elena and Dax sites, belonging to either the G1 or G2 fabric groups. The absence of this reflection indicates a firing temperature at least higher than 850 °C. The mineral assemblage identified by XRD suggests firing temperatures approximately 850 °C for most of the studied wares.

4.3. Chemical Analyses

The geochemical study was carried out on 143 samples. The studied samples are characterised by high content loss on ignition (LOI). High LOI values are usually attributed to the abundance of calcite or carbonate inclusions in the pottery. However, calcite or carbonate occurrence in these samples is restricted, thus the high LOI values can be attributed to postdepositional chemical modifications (Table 1). In addition, a high content of P_2O_5 (>0.3% wt) was detected in 70% of the samples analysed. These values are very high in comparison with raw clays, with average values of 0.15 wt% P_2O_5 for shales [49] and 0.23 wt% for greywackes [50,51]. The abundance of phosphorus in archaeological pottery

is often attributed to its adsorption from the soil during burial [52–56] or to the presence of the element in the raw material [57], although a few authors support the hypothesis of the contamination of pots by food during cooking or storage [58,59].

Table 1. Major and trace element chemical compositions of the studied G1, G2 and G3 pottery productions. Whole rock major oxides data (in weight percent) and trace element data (in parts per million).

Group Production	G1 (*n* = 63)			G2 (*n* = 44)			G3 (*n* = 36)		
	Av	Max	Min	Av	Max	Min	Av	Max	Min
SiO_2	63.32	76.02	46.79	64.79	73.68	56.01	63.64	71.52	53.63
Al_2O_3	15.26	18.59	11.73	13.75	17.91	10.29	16.63	24.43	11.66
TiO_2	0.64	0.91	0.32	0.62	1.38	0.38	0.64	0.99	0.32
CaO	2.17	6.30	0.00	1.05	2.03	0.00	1.90	4.22	0.38
Fe_2O_3	5.81	9.32	4.43	4.88	8.41	3.43	5.39	7.49	2.86
K_2O	2.18	3.18	0.68	2.20	3.08	1.41	2.58	3.38	1.38
MgO	1.06	1.44	0.37	0.75	2.18	0.34	0.99	1.73	0.37
MnO	0.08	0.27	0.02	0.09	0.18	0.03	0.08	0.20	0.02
Na_2O	0.56	1.27	0.00	0.50	1.33	0.14	0.84	1.43	0.32
P_2O_5	1.09	6.67	0.01	1.01	4.46	0.03	1.01	4.13	0.11
LOI	7.46	26.76	1.00	9.42	19.40	3.51	6.23	16.00	0.58
Ba	505	1226	94	490	887	309	520	1354	219
Hf	5.5	13.1	2.5	5.4	9.7	2.3	4.8	6.5	3.2
Nb	16.8	50.1	7.3	18.4	64.2	6.7	16.6	25.4	8.9
Rb	114	258	18	102	230	53	130	211	59
Sc	12.8	23.0	1.0	12.4	34.5	7.1	12.2	18.7	5.3
Sr	183	473	19	146	322	56	173	420	74
Th	12.3	15.7	9.9	10.8	16.0	8.1	13.0	20.3	9.8
U	2.5	4.9	1.7	2.1	3.8	1.1	3.3	9.3	2.2
V	113	179	36.6	78.0	262	26.7	116	172	74.1
Y	35.6	59.4	17.6	25.9	44.2	17.6	36.2	73.2	18.3
Zn	109	260	63.3	95.2	275	56.3	100	180	62.2
Zr	198	475	102	188	330	96.1	166	223	114
La	45.04	103.4	26.60	30.63	44.21	18.11	42.06	72.39	17.84
Ce	97.90	354.0	51.10	66.93	107.9	38.71	92.40	342.0	42.81
Pr	11.30	21.93	6.32	7.61	11.53	4.71	10.88	18.79	5.00
Nd	40.61	71.08	23.08	27.33	41.80	16.84	39.25	67.60	17.97
Sm	7.72	13.22	4.31	5.24	8.51	3.32	7.73	13.58	3.71
Eu	1.51	2.89	0.73	1.05	1.72	0.73	1.54	2.76	0.75
Gd	6.70	13.05	3.47	4.62	7.83	2.61	6.34	11.39	3.32
Tb	1.00	1.85	0.55	0.67	1.23	0.44	1.01	1.92	0.55
Dy	5.88	10.67	3.19	3.90	7.08	2.23	6.28	12.40	3.44
Ho	1.10	2.02	0.58	0.75	1.26	0.40	1.20	2.27	0.69
Er	3.03	5.46	1.55	2.06	3.60	1.07	3.13	5.54	2.00
Tm	0.46	0.79	0.22	0.31	0.53	0.15	0.51	0.87	0.32
Yb	2.94	4.78	1.46	2.05	3.49	0.95	3.13	5.25	2.02
Lu	0.46	0.74	0.22	0.32	0.52	0.14	0.50	0.80	0.32

Av.: average; Max.: maximum; Min: minimum; *n*: number of samples.

Chemical analysis by EDS coupled with the SEM indicates that even higher concentrations of phosphorus are found in the porous and crack systems, suggesting secondary precipitation during burial (Figure 8). This post-depositional chemical modification process is significant at various sites and influences the elemental chemical composition of pottery. Figure 9 shows the positive correlation between phosphorus, barium and strontium, with different patterns of correlation depending on the site of provenance of the wares. Such different variation patterns suggest a burial genesis related to a different geological environment rather than the use of the pieces for cooking food [60].
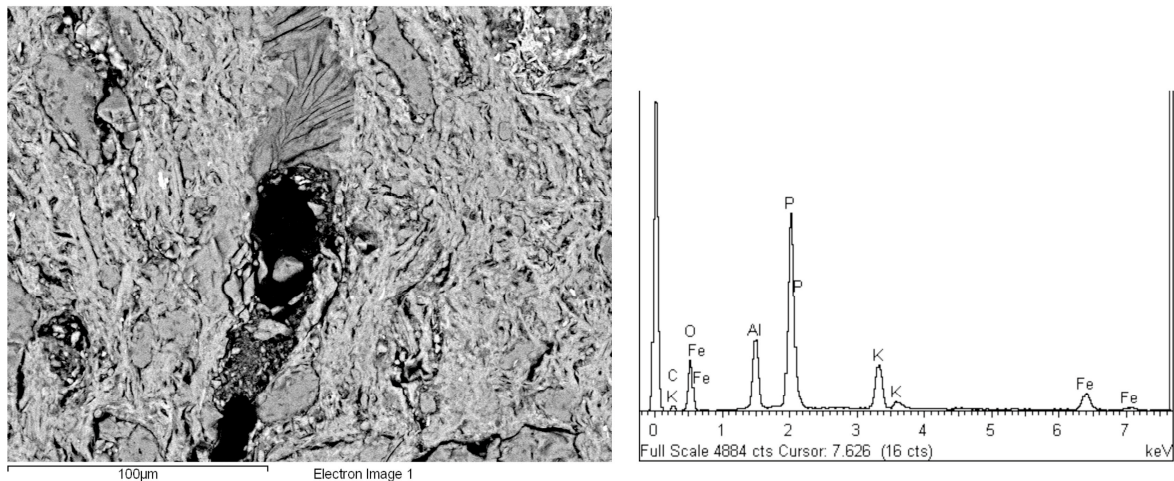
Figure 8. Scanning electron microscopy photomicrograph and elemental analysis (EDX) of fan-type habit phosphate aggregates filling a fracture.
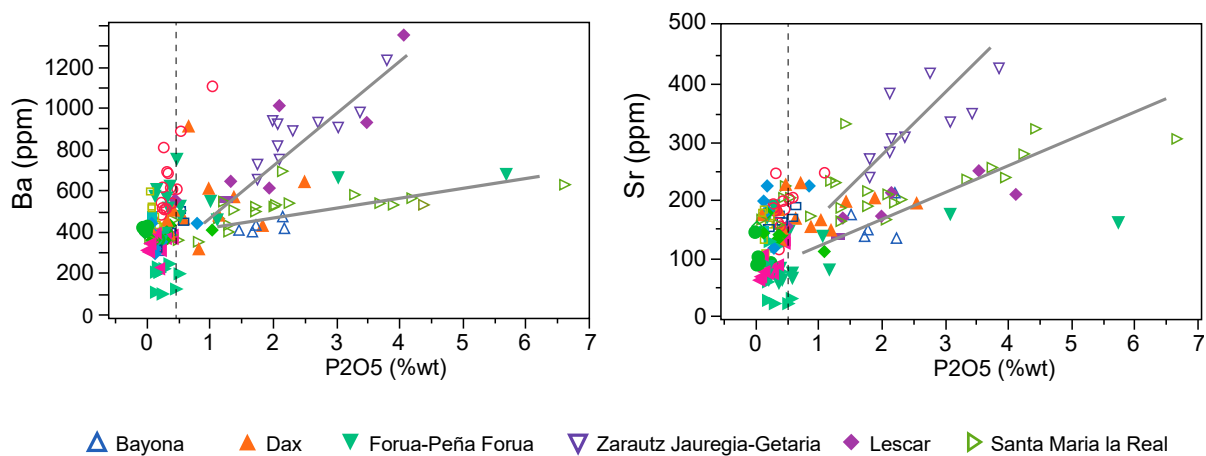
Figure 9. Bivariate plots of P_2O_5 vs. Sr and P_2O_5 vs. Ba show different correlations according to the archaeological site. Dotted line corresponds to the limit between modified and unmodified pottery samples.

A statistical approach was used to evaluate the results of chemical analyses, following the guidelines of Papageorgiou [61]. Different statistical techniques were used to explore sample patterning and assess chemical fingerprint significance. Ward's hierarchical clustering method and Euclidean distances were calculated after z-score normalisation to relate chemical sample groupings to archaeological classifications. In order to obtain significant chemical differences related to the raw material provenance or the mode of pottery production, it is essential to exclude samples that show a clear chemical modification due to burial.

Looking at the full set of samples in the cluster analysis, two clusters denoting two different chemical modification processes group samples with clear chemical modifications and mask the chemical characteristics of the samples. All samples with a phosphorus content of more than 0.5% by weight were excluded from the multivariate analysis. The excluded samples correspond mainly to the G1 fabric group from the Santa Maria la Real and Zarautz Jauregia sites and also to the Bayonne and Lescar sites in the G2 and G3 groups, respectively.

Multivariate analyses showed that the samples are clustered into three distinct groups, named A, B, and C (Figure 10). Two subgroups can be identified in Cluster A. One subgroup encloses early Roman Empire pottery, consisting mainly of wares of the G2 fabric group, corresponding to the TP 2.1 petrographic fabric. The second subgroup enclosed samples

from Santiagomendi, and most of the samples from the Santa Elena sites without a clear temporal assignment, but which are dated between the 3rd century BC and the 1st century AD [30,62]. These wares correspond to the G1 and G3 fabric groups.
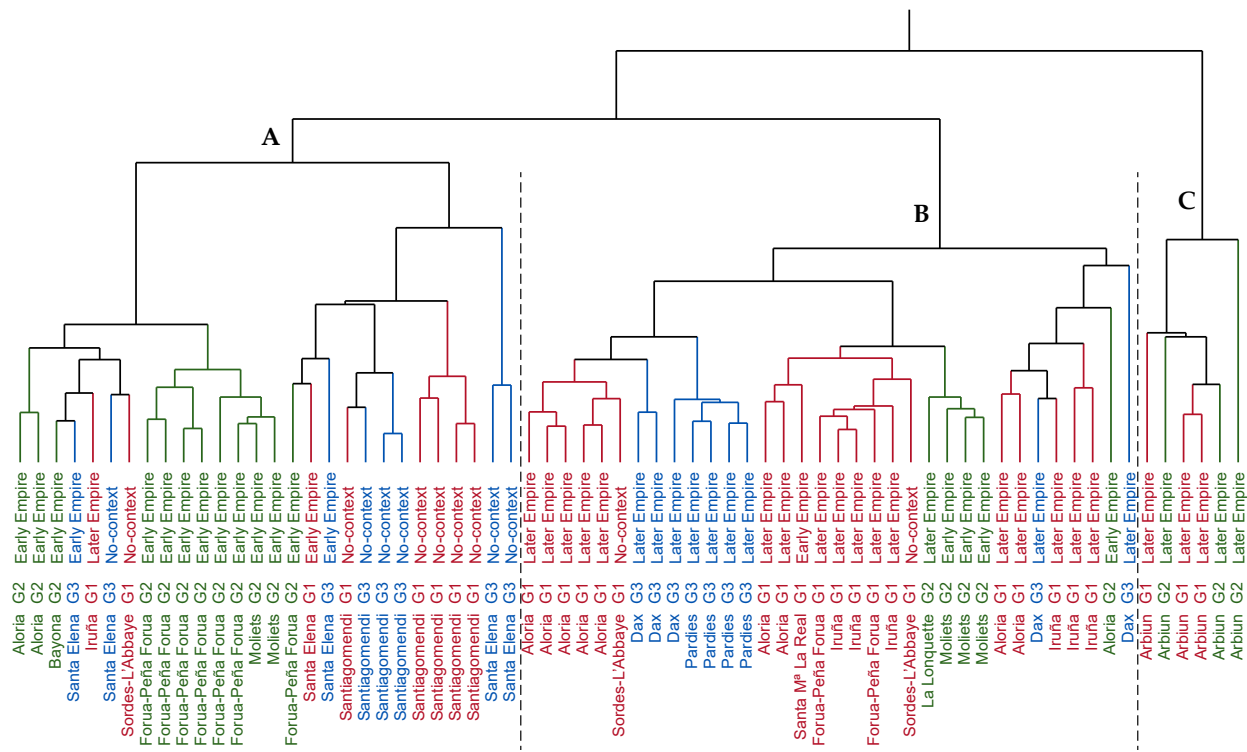

Figure 10. Hierarchical cluster analysis dendrogram based on Ward's method (according to Euclidean distances) for the significant variables. Colours correspond to fabric groups: red for the G1, green for the G2 and blue for the G3 fabric group. A, B and C represent cluster A, cluster B and cluster C.

Cluster B enclosed most of the pottery of the later Roman Empire age, including pottery from the G1, G2, and G3 fabric groups. Three subgroups can be distinguished according to fabric group and archaeological site in both the Tarraconensis and Aquitania Roman regions. Cluster C is defined by pottery from the Late Roman Arbium site, including samples of G1 and G2 fabric groups.

Principal component analysis (PCA) was carried out with the low P_2O_5 (<0.5% wt) content, i.e., the "*non modified*" chemical dataset. The analysis of the principal components, including major and trace elements, shows that the individuals in the main fabric groups do not pull apart significantly. Figure 11 shows G1 and G3 samples overlapped into one group and G2 samples were plotted separately.

The sum of the variance of the first two principal component axes is relatively low and accounted for 42.5% of the variance. The PCA score plot shows a concentration of samples belonging to the G2 fabric group, mainly corresponding to the TP 2.1 fabric, with negative values for PC1, due to the high LOI (Figure 11a). Other samples with a negative value for PC1 and a positive value for PC2 correspond to pottery mainly from the Santa Elena site, displaying different petrographic fabrics. The other samples of the G1 and G3 fabric groups are concentrated towards positive values for PC1, with higher contents of MgO, K_2O, Sr and REE associated with petrographic types enriched in clayey matrix (Figure 11b).
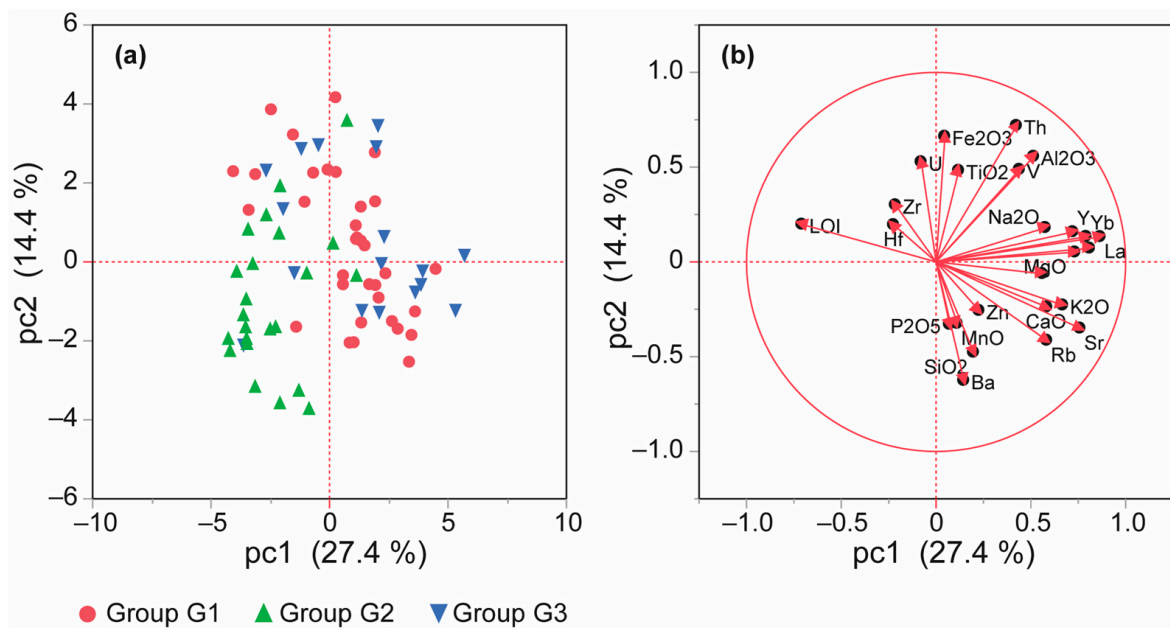
Figure 11. Principal component analysis of chemical data performed on the low P_2O_5 (<0.5% wt) content, i.e., the "*non modified*" chemical dataset of the three fabric groups. (**a**) Plot of pc1 versus pc2, representing 27% and 14% of total variance, respectively. (**b**) Loading plot of variables considered for pc1 versus pc2.

5. Discussion

Many pottery samples included in this study show evidence of chemical modification, sometimes severe, during burial. High contents of phosphorus, other trace elements (e.g., Ba and Sr) and LOI are indicative of this modification. Different chemical modification behaviours were observed depending on the fabric group. Despite the similarity in the phosphorus content of the three fabric groups (Table 1), the percentage of samples showing chemical modification signs is higher for the G2 (62%) in comparison to the G1 and G3 fabric groups (45%). Generally, the G2 groupwares display higher LOI contents too. The different behaviour of chemical modification during burial may be due to firing at low temperatures, according to experimental work by [63,64]. In this way, burial modifications make it problematic to use the chemical composition to establish the raw material provenance, diffusion, and trade of pottery. Conversely, the petrographic characteristics of the fabric remain unchanged during burial and reflect the original variations in raw material provenance.

The G1 fabric group, which is the most abundant, has a very widespread distribution. It is found in all the sites of the Tarraconensis Roman province and in the Aquitanian sites of the Lower Adour region (Bayonne, Dax and Sorde-l'Abbaye). With the exception of the samples from Bayonne and Santa Elena, which could be dated somewhat earlier, the chronological frame is mainly the later Roman Empire (3rd to 5th centuries). The petrographic characteristics indicate a careful treatment of the pastes, suggesting the existence of a pottery region or group of potters with a common area of raw material supply following similar technological procedures and recipes. The wide geographical distribution of this G1 fabric group indicates a very efficient and dynamic distribution network around the Bay of Biscay during the later Roman Empire.

Considering the geographical distribution of the pottery and the nature of the inclusions, it is possible to hypothesise about the provenance of the raw materials. The geological materials surrounding the studied sites in the Tarraconensis Roman province must be excluded as a source of raw materials. The occurrence of high-degree metamorphic rock inclusions within G1 wares rules out this region as the provenance area due to the absence of these rock types in the geological surroundings of the sites. The polygenic nature

of the inclusions within G1 indicates the provenance of sediments from a hydrographic basin, draining an orogenic chain with large lithological diversity. The central and western Pyrenees, where a wide variety of plutonic and metamorphic rocks crop out [31,32], are the most likely geological regions for this type of sediment. There are remarkable differences in the geology of the basins to the south and north of the Pyrenees. The southern basins of the Pyrenees are mainly composed of Mesozoic carbonate rocks, whereas medium- and high-grade metamorphic materials are absent and igneous rocks are minor [65]. In the northern basin, in addition to Mesozoic carbonates, the Paleocene-Oligocene and Quaternary siliciclastic sediments are the more abundant and widespread materials, as well as various medium- and high-grade metamorphic rocks and granitoid rocks (Figure 12; Table S2). The Adour River and its southern tributaries erode and transport this type of material, and in the lower reaches of its basin, there are several archaeological sites where G1 fabric pottery predominates. Therefore, based on the petrographic characteristics of the G1 group and the criterion of abundance [66] of these G1 vessels, the most likely provenance area of the raw material was the lower Adour basin, from where it was distributed around the Bay of Biscay and scattered towards the interior, reaching the upper Ebro Valley [29,67]. Moreover, recent studies of similar wares with a comparable composition in the Ebro Valley [68] indicate that further research is needed to unravel the provenance of this production ware, suggesting a wider production area in the surroundings of the Pyrenees.
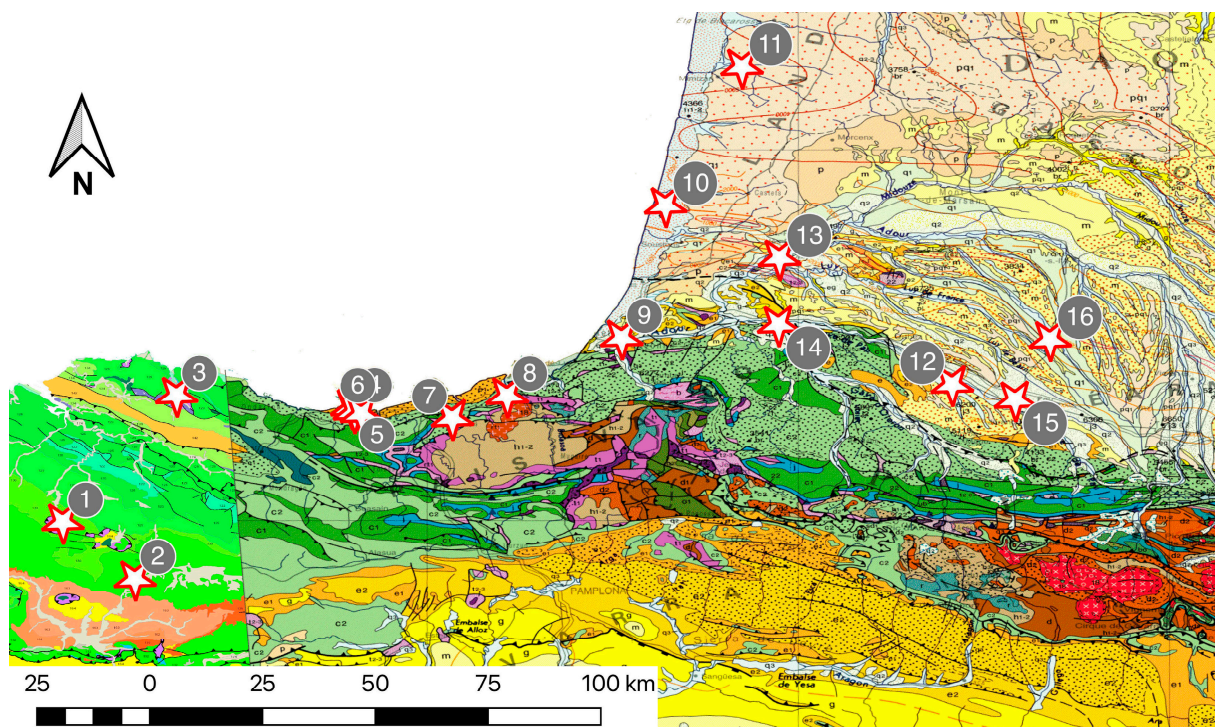
Figure 12. Geological map of the studied region. Brown: Palaeozoic and Permian; Pink: Palaeozoic Ursuya massif; Red: granitoids; Purple: Triassic; Blue: Jurassic; Green: Cretaceous; Orange: Paleogene; Yellow: Eocene; Light brown and Grey: Quaternary. Stars indicate the location of the sites: 1: Aloria, 2: Iruña-Veleia, 3: Forua-Peña Forua, 4: Getaria-Zarautz Jauregia, 5: Arbium 6: Santa Maria la Real, 7: Santiagomendi, 8: Santa Elena, 9: Bayonne, 10: Moliets, 11: Saint-Paul-en-Born, 12: Pardies, 13: Dax, 14: Sordes l'Abbaye, 15: Lescar, 16: Lalonquete. The geological maps of Spain and France are available at the Spanish (IGME) and French Geological Survey (BRGM) geological services [69,70].

G2 group pottery displays a clear coastal distribution around the Bay of Biscay. These potteries are mainly found at the sites of Bayonne and Moliets in Aquitania province and at Santa Elena, Santa Maria la Real, Arbiun, Getaria-Zarautz Jauregia and Forua and Aloria sites in Tarraconensis province. Chronologically, they correspond to the early

Roman Empire (1st–2nd century), although some samples have been found in later Roman archaeological contexts at the geographically very close sites of Arbiun, Getaria-Zarautz Jauregia and Santa Maria la Real [29].

The G2 fabric group was geographically distributed in both provinces in the early Roman period. Petrographically, it is more homogeneous than the G1 group. Thus, the petrographic fabric TP 2.1 occurs at Tarraconensis sites, whereas the fabric TP 2.2 occurs at Aquitania sites, although recent unpublished studies recognise the occurrence of TP 2.1 fabric at several Aquitanian sites. In addition, some wares of TP 2.1 fabric show graffiti attributed to the potter [34,71]. As with the previous G1 pottery, the petrographic fabric of the G2 group indicates that the raw materials must be linked to the areas where plutonic and high-grade metamorphic rocks occur; thus, the sediments used as raw materials originated from the Axial Zone or central Pyrenees. The Palaeozoic Ursuya Massif in the westernmost Pyrenees, which includes diorite plutonic and high-grade metamorphic rocks [72] and is drained by the Nive River and its tributaries, may be the most likely source area for the raw material. In addition, the grain size heterogeneity and high angularity of the inclusions indicate a provenance area from the middle-upper Nive River basin (Figure 12; Table S2). Although the provenance area of the raw material can be attributed to the Nive River basin, the regional geographical distribution of the petrographic fabrics suggests several production centres with different supply areas. The production centres for these ceramics must therefore be located in southern Aquitania.

The pottery of the G3 fabric group is the most heterogeneous, as shown by the wide variety of petrographic fabrics, and has been found in both Aquitania and Tarraconensis provinces. Chronologically, it corresponds to the early Roman period (1st–2nd century) at the sites of Lescar, Pardies (Aquitania) and Santa Elena, Santiagomendi sites (Tarraconensis), and to the Late Roman period (4th–5th century) for most of the pottery at the Dax site. In most cases, each of the petrographic fabrics has been found at a single archaeological site, suggesting a local provenance of the raw material for each site (Figure 12; Table S2). Most of the TP 3.1 wares were found at the Dax site and are characterised by polycrystalline chessboard-patterned quartz inclusions. These microstructures were described for Lys and Néouvielle pluton lithologies within the axial zone of the Pyrenees at the headwaters of the Adour River [31,32]. The Adour River then transported the sediments formed by the weathering and erosion of these materials to the middle or lower reaches of the river, where the raw material supply area was located. The TP 3.2 petrographic fabric is the most common and is found at sites on both sides of the Pyrenees. The occurrence of idiomorphic plagioclase indicates that the sediments were formed close to the plutonic areas. Therefore, the raw material supply area can probably be located in the western Pyrenees within the Adour River basin, although the Oiartzun or Bidasoa River basins cannot be excluded [31]. The petrographic fabrics TP 3.3 and TP 3.5 occur only at Tarraconensis sites. The high sphericity and high roundness of the quartz grains occurring in TP 3.3 indicate that the raw material supply can be the coastal dune deposits consistent with the Landes region bordering the Bay of Biscay in the Aquitania Basin. The decanted fabric without the temper of the TP 3.5 makes tracing the provenance difficult. The fabric TP 3.4 occurs only at the Lescar site in Aquitania. The large grain size, high angularity and polygenic nature of the inclusions of this fabric suggest a source of raw material close to the river headwaters. The local sediments formed in the upper basin of the Gave de Pau (tributary of the Adour) can be considered a raw material source for this pottery. The fabric TP 3.6 was restricted to the Dax site. As in the previous case, the low frequency and limited distribution of the vessels and the fabric characteristics suggest the use of local clays compatible with the Adour deposits that dominate this area.

The studied pottery appears at sites associated with maritime, land or fluvial communication routes, both coastal and terrestrial. The production of G1 pottery was widespread in the studied region around the Bay of Biscay, with the greatest production and diffusion during the Later Empire times. Although G1 pottery production started in the Early Empire, it was not until the Later Empire that it became regionally widespread. The homogeneity

of this type of fabric indicates careful processing of the raw materials, suggesting a pottery workshop complex located in southern Aquitania. The good quality of the pottery and the development of robust trade networks favoured its widespread distribution, as evidenced by the profuse occurrence of these wares around the Bay of Biscay from Galicia to Bordeaux, and by the inland trade along the Ebro River as far as Saragossa [28,67,73–75].

The production of the G2 pottery group occurred mainly in the Early Empire period, although some samples were found in Later Empire contexts. The slight textural variability suggests a common technological tradition with small variations in the pottery's manufacture and slight differences in the provenance of raw materials from the western Pyrenees, in southern Aquitania during the early Roman period. Furthermore, the restricted distribution of this production on coastal sites suggests a preferential geographical distribution over inland areas.

The G3 pottery group occurs in two periods, during the Early Empire and at the end of the Later Empire. This production displays a limited and heterogeneous distribution network, occurring mainly in the Aquitania sites and in some of the easternmost sites of the Tarraconensis province. Local raw material provenance indicates local pottery production using similar technological patterns. Local productions suggest systems of trade networks that were not yet consolidated in the Early Empire, while in the Later Empire there was a weakening of the trade networks, coinciding with the crisis at the end of the empire, leading to their deconstruction and a re-localisation of pottery production.

6. Conclusions

The use of chemical composition in pottery provenance and diffusion studies should be taken with caution, as the composition may have undergone modifications either by the use of the pottery or by burial processes. The present study of pottery from several sites displays different patterns of chemical modification, limiting their use as a tool for studying their provenance and diffusion. Nevertheless, the mineralogical and microstructural composition of the fabrics does not change during burial, reflecting the original features of the raw materials and allowing the identification of provenance areas and trade networks.

The petrography study has also been applied to the common non-wheel thrown pottery from the Roman Aquitania-Tarraconensis provinces (CNT-AQTA), enabling the establishment of diffusion and trade patterns during Roman times around the Bay of Biscay. Technological persistence in pottery production traditions was observed throughout the Roman Empire. Variations in both the distribution patterns and the provenance areas of pottery during Roman times have also been identified.

The chronology of the manufacture and spread of CNT-AQTA pottery begins locally in Aquitania. Then, during the Early Empire, pottery of the G2 group was manufactured in several production centres in southern Aquitania following the same technological tradition. This ware production was the most widespread but restricted to coastal sites, suggesting a well-consolidated distribution network but limited to maritime traffic around the Bay of Biscay. During the Later Empire period, G1 pottery production was predominant and widely distributed both along the coast and in inland territories in the provinces of Aquitania and Tarraconensis. These wares were manufactured in the centres of production in southern Aquitania and/or a broader region surrounding the Pyrenees and widely distributed through a well-established trade network. Finally, during the final period of the later Roman Empire, locally manufactured G3 pottery was produced, preserving the technological tradition but with a reduced distribution and commercial capacity, closer to the Aquitania region and the easternmost Tarraconensis sites, reflecting the deterioration of the trade networks.

References

1. Costin, C.L. Production and Exchange of Ceramics. In *Empire and Domestic Economy*; D'Altroy, T.N., Hastorf, C.A., Eds.; Springer: Boston, MA, USA, 2002; pp. 203–242.
2. Sillar, B. Reputable pots and disreputable potters: Individual and community choice in present-day pottery production and exchange in the Andes. In *Not So Much a Pot, More a Way of Life: Current Approaches to Artefact Analysis in Archaeology*; Cumberpatch, C., Blinkhorn, P., Eds.; Oxbow Books Ltd.: Oxford, UK, 1997; pp. 1–20.
3. Tite, M.S. Pottery Production, Distribution, and Consumption—The Contribution of the Physical Sciences. *J. Archaeol. Method Theory* **1999**, *6*, 181–233. [CrossRef]
4. Réchin, F. La Vaisselle Commune d'Aquitaine Méridionale à L'époque Romaine: Contexte Céramique, Typologie, Diffusion, Faciès de Consommation. Ph.D. Thesis, Université de Pau et des Pays d'Adour, Pau, France, 1994.
5. Santrot, M.-H.; Santrot, J. *Céramiques Communes Gallo-Romaines d'Aquitaine*; CNRS: Paris, France, 1979.
6. Esteban, M. Yacimiento de Arbiun (Zarautz): I Campaña de excavaciones. *Arkeoikuska Investig. Arqueol.* **1993**, *1993*, 214–217.
7. Martínez Salcedo, A.; Unzueta, M. Forua: Un Asentamiento Romano en la ría de Gernika (Vizcaya). In *Los Orígenes de la Ciudad en el Noroeste Hispánico*; Rodríguez Colmenero, A., Ed.; Servicio de Publicaciones de la Diputación Provincial: Lugo, Spain, 1999; pp. 523–534.
8. Gil Zubillaga, E. Ciudad de Iruña/Veleia (Iruña de Oca). *Arkeoikuska Investig. Arqueol.* **1995**, *1995*, 101–110.
9. Cepeda, J.J. Asentamiento romano de Aloria (Arrastaria, Álava; Orduña, Bizkaia): V Campaña de excavaciones. *Arkeoikuska Investig. Arqueol.* **1994**, *1994*, 132–140.
10. Cepeda, J.J. *La Romanización en los Valles Cantábricos Alaveses: El Yacimiento Arqueológico de Aloria*; Museo de Arqueología de Álava: Vitoria-Gasteiz, Spain, 2001.
11. Núñez Marcén, J.; Cepeda, J.J.; Esteban Delgado, M.; Filloy Nieva, I.; Garía Garía, M.L.; Gil Zubillaga, E.; Hernández Vera, J.A.; Martínez Salcedo, A.; Ruiz Gutiérrez, A.; Réchin, F. La romanización en el Cantábrico Oriental. In *Medio Siglo de Arqueología en el Cantábrico Oriental y su Entorno*; Instituto Alavés de Arqueología, Diputación Foral de Alava: Vitoria-Gasteiz, Spain, 2009; pp. 345–448.
12. Martínez Salcedo, A. Apunte para el estudio de las cerámicas comunes no torneadas de época romana en el País Vasco peninsular: El caso de las ollas peinadas de borde vuelto plano. *Kobie* **1999**, *25*, 161–182.
13. de Soto, P. Network Analysis to Model and Analyse Roman Transport and Mobility. In *Finding the Limits of the Limes: Modelling Demography, Economy and Transport on the Edge of the Roman Empire*; Verhagen, P., Joyce, J., Groenhuijzen, M.R., Eds.; Springer International Publishing: Cham, Switzerland, 2019; pp. 271–289.
14. Roldán, J.M. *Itineraria Hispana: Fuentes Antiguas para el Estudio de las vías Romanas en la Península Ibérica*; Departamento de Historia Antigua, Universidad de Valladolid: Madrid, Spain, 1975; p. 279.
15. Ruiz-Gutiérrez, A. La costa cantábrica, un espacio de circulación e intercambios en el Imperio romano. In *Anejos de Oppidum. Estudios y Recuerdos in Memoriam Prof. Emilio Illarregui Gómez*; Pérez González, C., Arribas Lobo, P., Reyes Hernando, O.V., Eds.; IE Universidad: Segovia, Spain, 2020; Volume 7, pp. 135–146.
16. Esteban Delgado, M.; Izquierdo Marculeta, M.T.; Martínez Salcedo, A. La cerámica de Época Romana en el País Vasco Atlántico: Redes comerciales y consumo. In *Cerámicas de Época Romana en el Norte de Hispania y en Aquitania. Producción, Comercio y Consumo Entre el Duero y el Garona*; Martínez Salcedo, A., Esteban Delgado, M., Alcorta Irastorza, E., Eds.; La Ergástula: Madrid, Spain, 2015; Volume 1, pp. 193–210.
17. Fernández Ochoa, C.; Morillo Cerdan, Á. La ruta marítima del Cantábrico en época romana. *Zephyrvs* **2009**, *46*, 225–232.

18. Morillo Cerdan, A.; Fernández Ochoa, C. *De Brigantium a Oiasso. Aproximación al Estudio de los Enclaves Marítimos Cantábricos en Época Romana*; Foro. Arqueología, Proyectos y Publicaciones S.L.: Madrid, Spain, 1994; Volume 3.

19. Fernández Fernández, A.; Folgueira Castro, A.; Alcorta Irastorza, E. Horizontes cerámicos tardoantiguos en Punta Atalaia (Cervo-Lugo). Una revisión del comercio cantábrico entre los siglos IV y VI. *Anejos Nailos Estud. Interdiscip. Arqueol.* **2019**, *5*, 551–602.

20. de Soto, P. Los sistemas de transporte romanos y la configuración territorial en el noroeste peninsular. In *O Irado Mar Atlântico. O Naufragio Bético Augustano de Esposende (Norte de Portugal)*; Morais, R., Graja, H., Morillo, A., Eds.; Museo de Arqueologia Diogo de Sousa: Braga, Portugal, 2013; pp. 1–15.

21. Martínez Salcedo, A.; Unzueta Portilla, M. La "via maris" y el poblamiento costero en Vizcaya. In *Gijón, Puerto Romano: Navegación y Comercio en el Cantábrico Durante la Antigüedad*; Fernández Ochoa, C., Ed.; Lunwerg: Barcelona, Spain, 2003; pp. 162–177.

22. Esteban Delgado, M. La vía marítima en época antigua, agente de transformación en las tierras costeras entre Oiasso y el Divae. *Itsas Mem. Rev. Estud. Marítimos País Vasco* **2003**, *4*, 13–40.

23. Izquierdo Marculeta, M.T.; Esteban Delgado, M. Acerca de la costa cantábrica, el bajo Urumea en época antigua y el Morogi pliniano. *Munibe Antropol.-Arkeol.* **2005**, *57*, 389–404.

24. Peña-Chocarro, L.; Zapata, L. Trade and New Plant Foods in the Western Atlantic Coast: The Roman Port of Irun (Basque Country). In *Mar Exterior, el Occidente Atlántico en Época Romana, Proceedings of the El Occidente Atlántico en Época, Pisa, Italy, 6–9 November 2003*; Urteaga Artigas, M.M., Noain Maura, M.J., Eds.; Escuela Española de Historia y Arqueología en Roma-CSIC: Madrid, Spain, 2005; pp. 169–193.

25. Pena-Chocarro, L.; Zapata, L.; Iriarte, M.J.; Morales, M.G.; Straus, L.G. The oldest agriculture in northern Atlantic Spain: New evidence from EL Miron Cave (Ramales de la Victoria, Cantabria). *J. Archaeol. Sci.* **2005**, *32*, 579–587. [CrossRef]

26. Martin Bueno, M.A.; Salis, J.R. The anchorage of El Cabo de Higuer (Fuenterrabía, Guipúzcoa). *Int. J. Naut. Archaeol.* **1975**, *4*, 331–333. [CrossRef]

27. Esteban, M.; Izquierdo, M.T.; Martínez Salcedo, A.; Réchin, F. Producciones de cerámica común no torneada en el País Vasco peninsular y Aquitania meridional: Grupos de producción, tipología y difusión. *Sautuola Rev. Inst. Prehist. Y Arqueol. Sautuola* **2008**, *14*, 183–216.

28. Aguarod, M.C. La cerámica común de producción local/regional e importada. Estado de la cuestión en el valle del Ebro. In *Ceràmica Comuna Romana d' Època Alto-Imperial a la Península Ibèrica: Estat de la Qüestió*; Aquilué, X., Roca, M.M., Eds.; Museu d'Arqueologia de Catalunya: Empúries, Spain, 1995; pp. 129–153.

29. Esteban, M.; Martínez Salcedo, A.; Ortega, L.A.; Alonso-Olazabal, A.; Izquierdo, M.T.; Rechin, F.; Zuluaga, M.C. *La Cerámica común Romana no Torneada de Difusión Aquitano-Tarraconense (s. II a. C-s. V d. C.): Estudio Arqueológico y Arquemétrico*; Bizkaiko Foru Aldundia: Bilbao, Spain, 2012; Volume 12, p. 270.

30. Ceberio, M. Nuevas aportaciones al estudio de la transición de la edad del hierro a época romana en Gipuzkoa: El caso de Santiagomendi (Astigarraga). *Munibe Antropol.-Arkeol.* **2009**, *60*, 219–241.

31. Debon, F.; Enrique, P.; Autran, A. Magmatisme hercynien. In *Synthèse Géologique et Géophysique des Pyrénées*; Barnolas Cortinas, A., Chiron, J.C., Guérangé, B., Eds.; BRGM/ITGE: Orléans, France, 1996; Volume 1, pp. 361–499.

32. Guitard, G.; Vielzeuf, D.; Martinez, F. Le Métamorphisme Hercynien. In *Synthèse Géologique et Géophysique des Pyrénées*; Barnolas Cortinas, A., Chiron, J.C., Guérangé, B., Eds.; BRGM/ITGE: Orleans, France; Madrid, Spain, 1995; Volume 1, pp. 501–584.

33. Tugend, J.; Manatschal, G.; Kusznir, N.J.; Masini, E.; Mohn, G.; Thinon, I. Formation and deformation of hyperextended rift systems: Insights from rift domain mapping in the Bay of Biscay-Pyrenees. *Tectonics* **2014**, *33*, 1239–1276.

34. Martínez Salcedo, A. *La Cerámica Común de Época Romana en el País Vasco: Vajilla de Cocina, mesa y Despensa Procedente de los Asentamientos de Aloria (Álava), Forua (Bizkaia) e Iruña/Veleia*, 1st ed.; Servicio Central de Publicaciones del Gobierno Vasco: Vitoria-Gasteiz, Spain, 2004; p. 470.

35. Riederer, J. Thin Section Microscopy Applied to the Study of Archaeological Ceramics. *Hyperfine Interact.* **2004**, *154*, 143–158. [CrossRef]

36. Reedy, C.L. *Thin-Section Petrography of Stone and Ceramic Cultural Materials*; Archetype Publications: Plymouth, UK, 2008; p. 256.

37. Compon, R. *Manual of Field Geology*; John Wiley & Sons: New York, NY, USA, 1962; p. 378.

38. Whitbread, I.K. The characterisation of argillaceous inclusions in ceramic thin sections. *Archaeometry* **1986**, *28*, 79–88. [CrossRef]

39. Whitbread, I.K. *Greek Transport Amphorae: A Petrological and Archaeological Study*; British School at Athens: Athens, Greece, 1995; p. 453.

40. García de Madinabeitia, S.; Sánchez Lorda, M.E.; Gil Ibarguchi, J.I. Simultaneous determination of major to ultratrace elements in geological samples by fusion-dissolution and inductively coupled plasma mass spectrometry techniques. *Anal. Chim. Acta* **2008**, *625*, 117–130. [CrossRef]

41. Whitney, D.L.; Evans, B.W. Abbreviations for names of rock-forming minerals. *Am. Mineral.* **2010**, *95*, 185–187. [CrossRef]

42. Velraj, G.; Janaki, K.; Musthafa, A.M.; Palanivel, R. Estimation of firing temperature of some archaeological pottery shreds excavated recently in Tamilnadu, India. *Spectrochim. Acta Part A-Mol. Biomol. Spectrosc.* **2009**, *72*, 730–733. [CrossRef]

43. Cultrone, G.; Rodriguez-Navarro, C.; Sebastian, E.; Cazalla, O.; De La Torre, M.J. Carbonate and silicate phase reactions during ceramic firing. *Eur. J. Mineral.* **2001**, *13*, 621–634. [CrossRef]

44. Trindade, M.J.; Dias, M.I.; Coroado, J.; Rocha, F. Mineralogical transformations of calcareous rich clays with firing: A comparative study between calcite and dolomite rich clays from Algarve, Portugal. *Appl. Clay Sci.* **2009**, *42*, 345–355. [CrossRef]

45. Trindade, M.J.; Dias, M.I.; Coroado, J.; Rocha, F. Firing tests on clay-rich raw materials from the Algarve basin (Southern Portugal): Study of mineral transformations with temperature. *Clays Clay Miner.* **2010**, *58*, 188–204. [CrossRef]

46. Tschegg, C.; Ntaflos, T.; Hein, I. Thermally triggered two-stage reaction of carbonates and clay during ceramic firing—A case study on Bronze Age Cypriot ceramics. *Appl. Clay Sci.* **2009**, *43*, 69–78. [CrossRef]

47. Kramar, S.; Lux, J.; Mladenović, A.; Pristacz, H.; Mirtič, B.; Sagadin, M.; Rogan-Šmuc, N. Mineralogical and geochemical characteristics of Roman pottery from an archaeological site near Mošnje (Slovenia). *Appl. Clay Sci.* **2012**, *57*, 39–48. [CrossRef]

48. Rathossi, C.; Pontikes, Y. Effect of firing temperature and atmosphere on ceramics made of NW Peloponnese clay sediments. Part I: Reaction paths, crystalline phases, microstructure and colour. *J. Eur. Ceram. Soc.* **2010**, *30*, 1841–1851. [CrossRef]

49. Taylor, S.R.; McLennan, S.M. *The Continental Crust: Its Composition and Evolution: An Examination of the Geochemical Record Preserved in Sedimentary Rocks*; Blackwell Scientific: Oxford, UK, 1985; p. xv. 312p.

50. Floyd, P.A.; Shail, R.; Leveridge, B.E.; Franke, W. Geochemistry and provenance of Rhenohercynian synorogenic sandstones: Implications for tectonic environement discrimination. In *Developements in Sedimentary Provenance Studies*; Morton, A.C., Tood, S.P., Haughton, P.D.W., Eds.; The Geologial Society: London, UK, 1991; Volume 57, pp. 173–188.

51. Wedepohl, K.H. *Handbook of Geochemistry*; Springer: Berlin, Germany, 1969; Volume 1, pp. 1–442.

52. Maritan, L.; Angelini, I.; Artioli, G.; Mazzoli, C.; Saracino, M. Secondary phosphates in the ceramic materials from Frattesina (Rovigo, North-Eastern Italy). *J. Cult. Herit.* **2009**, *10*, 144–151. [CrossRef]

53. Maritan, L.; Mazzoli, C. Phosphates in archaeological finds: Implications for environmental conditions of burial. *Archaeometry* **2004**, *46*, 673–683. [CrossRef]

54. Freestone, I.C.; Meeks, N.D.; Middleton, A.P. Retention of phosphate in buried ceramics: An electron microbeam approach. *Archaeometry* **1985**, *27*, 161–177. [CrossRef]

55. Maritan, L. Ceramic abandonment. How to recognise post-depositional transformations. *Archaeol. Anthropol. Sci.* **2020**, *12*, 199–219.

56. Schneider, G. Mineralogical and Chemical Alteration. In *The Oxford Handbook of Archaeological Ceramic Analysis*; Hunt, A., Ed.; Oxford University Press: New York, NY, USA, 2016; pp. 162–180.

57. Ionescu, C.; Hoeck, V.; Ghergari, L. Electron microprobe analysis of ancient ceramics: A case study from Romania. *Appl. Clay Sci.* **2011**, *53*, 466–475. [CrossRef]

58. Rodrigues, S.F.S.; da Costa, M.L. Phosphorus in archeological ceramics as evidence of the use of pots for cooking food. *Appl. Clay Sci.* **2016**, *123*, 224–231. [CrossRef]

59. Costa, M.L.d.; Kern, D.C.; Pinto, A.H.E.; Souza, J.R.d.T. The ceramic artifacts in archaeological black earth (terra preta) from lower Amazon region, Brazil: Chemistry and geochemical evolution. *Acta Amaz.* **2004**, *34*, 375–385. [CrossRef]

60. Picon, M. La fixation du baryum et du strontium par les céramiques. *ArchéoSciences Rev. D'archéométrie* **1987**, *11*, 41–47. [CrossRef]

61. Papageorgiou, I. Ceramic investigation: How to perform statistical analyses. *Archaeol. Anthropol. Sci.* **2020**, *12*, 210–229. [CrossRef]

62. Izquierdo, M.T. El poblamiento de la Edad del Hierro en el entorno de Santiagomendi (Astigarraga, Guipúzcoa). In *Kobie: Homenaje al Profesor Dr. Juan Mª Apellániz, 30 años de Arqueología (1972–2002)*; Diputacion Foral de Bizkaia: Bilbao, Spain, 2004; Volume 1, pp. 297–304.

63. Dufournier, D.; Bearat, H. Quelques expériences sur la fixation du phosphore par les céramiques. *Rev. D'archéométrie* **1994**, *18*, 65–73.

64. Lemoine, C.; Picon, M. La fixation du phosphore par les céramiques lors de leur enfouissement et ses incidences analytiques. *Rev. D'archéométrie* **1982**, *6*, 101–112. [CrossRef]

65. Vera Torres, J.A.; Eumenio Ancochea, S. *Geología de España*; IGME: Madrid, Spain, 2004; p. 884.

66. Bishop, R.L.; Rands, R.L.; Holley, G.R. Ceramic compositional analysis in archaeological perspective. In *Advances in Archaeological Method and Theory*; Elsevier: Amsterdam, The Netherlands, 1982; pp. 275–330.

67. Alonso-Olazabal, A.; Martínez Salcedo, A.; Esteban Delgado, M.; Izquierdo, M.T.; Ortega, L.A.; Zuluaga, M.C.; Réchin, F. Archaeometry of Roman Aquitania-Tarraconensis coarse ware pottery from the northern Iberian Peninsula and southern Aquitania. *Antiquity* **2018**, *92*, e7. [CrossRef]

68. Aguarod, M.C. (University of Zaragoza, Zaragoza, Spain); LApuente, M.P. (University of Zaragoza, Zaragoza, Spain). Recent studies of similar wares with a comparable composition in the Ebro valley indicate that further research is needed to unravel the provenance of this production ware suggesting a wider production area in the surroundings of the Pyrenees. Personal Communication, 2023.

69. Rodríguez Fernández, L.R.; López Olmedo, F.; Oliveira, J.T.; Medialdea, T.; Terrinha, P.; Matas, J.; Martín-Serrano, A.; Martín Parra, L.M.; Rubio, F.; Marín, C.; et al. Mapa Geológico de la Península Ibérica, Baleares y Canarias a Escala 1:1.000.000, 2015. ©Instituto Geológico y Minero de España (IGME). Available online: http://info.igme.es/cartografiadigital/geologica/Geologicos1MMapa.aspx?Id=Geologico1000_(2015)&language=es (accessed on 13 April 2023).

70. Chantraine, J.; Autran, A.; Cavelier, C. Carte géologique metropolitaine à 1/1 000 000, 2003. Bureau de Recherches Géologiques et Minières (BRGM). Available online: https://infoterre.brgm.fr/formulaire/telechargement-carte-geologique-metropolitaine-11-000-000 (accessed on 13 April 2023).

71. Fernández Vega, P.A.; Ramos Sáinz, M.L.; Ruiz-Gutiérrez, A. Marcas de fábrica sobre material de construcción cerámico en la Cantabria romana. *Sautuola Rev. del Inst. de Prehist. Y Arqueol. Sautuola* **2009**, *15*, 299–309.

72.   Boissonnas, J.; Le Pochat, G.; Thibault, C.; Bernatzky, M. *Carte Géologique de la France à 1:50,000. 1027 Iholdy*; Map Memory and Mapping; BRGM: Orléans, France, 1974; p. 32.

73.   Fernández Ochoa, C.; Zarzalejos Prieto, M.M. Reflexiones sobre un producción peculiar de cerámica común localizada en el tercio norte de la Península Ibérica y el sur de Aquitania: Los materiales de la ciudad de Gijón (España). *Cuad. Prehist. Y Arqueol.* **1999**, *25*, 251–266.

74.   Alcorta Irastorza, E. *Cerámica Común Romana de Cocina y mesa Hallada en las Excavaciones de la Ciudad*; Fundación Pedro Barrié de la Maza: A Coruña, Spain, 2001; p. 484.

75.   Barbazán Domínguez, S.; Ramil Rego, E.; Lozano Hermida, H. La evolución cronológica del Castro de Viladonga (Castro de Rei, Lugo) a través del estudio de su cerámica común romana. *BSAA Arqueol.* **2018**, *84*, 168–214. [CrossRef]